

NASA Contractor Report 3389

NASA
CR
3389
c.1

A Three-Dimensional Turbulent Compressible Subsonic Duct Flow Analysis for Use With Constructed Coordinate Systems

R. Levy, H. McDonald, W. R. Briley,
and J. P. Kreskovsky

CONTRACT NAS3-21735
APRIL 1981

NASA

LOAN COPY
AFWU TECHN
KIRTLAND AFB

0062260

TECH LIBRARY KAFB, NM



NASA Contractor Report 3389

A Three-Dimensional Turbulent Compressible Subsonic Duct Flow Analysis for Use With Constructed Coordinate Systems

R. Levy, H. McDonald, W. R. Briley,
and J. P. Kreskovsky
Scientific Research Associates, Inc.
Glastonbury, Connecticut

Prepared for
Lewis Research Center
under Contract NAS3-21735



National Aeronautics
and Space Administration

**Scientific and Technical
Information Branch**

1981

TABLE OF CONTENTS

	<u>Page</u>
SUMMARY	1
INTRODUCTION	2
ANALYSIS	3
Coordinate Systems	3
Governing Equations	5
Flow in Ducts with Superelliptic Cross Sections	9
Potential Flow	13
Calculations	14
SUMMARY AND CONCLUSIONS	16
REFERENCES	17
FIGURES	18
SYMBOL TABLE	28
APPENDIX - COMPUTER CODE INPUT AND OUTPUT	29

SUMMARY

An approximate analysis is presented for computation of three-dimensional subsonic flow in straight and curved diffusers. The development parallels that of Briley and McDonald for forward-marching solution of viscous primary and secondary flows, but differs in the coordinate formulation used and in details of the approximations. The present formulation is intended to facilitate the use of constructed coordinates in circumstances where it is difficult to maintain smooth behavior in higher derivatives. This analysis is applicable to nonorthogonal coordinate systems having a curved centerline and planar transverse coordinate surfaces normal to the centerline. The primary flow direction is taken to coincide with the local direction of the duct centerline and is hence normal to transverse coordinate planes. The formulation utilizes vector components (velocity, vorticity, transport equations) defined in terms of local Cartesian directions aligned with the centerline tangent, although the governing equations themselves are expressed in general nonorthogonal coordinates. For curved centerlines, these vector quantities are redefined in new local Cartesian directions at each streamwise location. The use of local Cartesian variables and fluxes leads to governing equations which require only first derivatives of the coordinate transformation, and this provides for the aforementioned ease in using constructed coordinates. The analysis is applied to a particular family of duct and diffuser geometries having curved centerlines and superelliptic cross sections, using a nonorthogonal constructed coordinate system. Present computed results are compared with available experimental measurements for different but related flow conditions. Qualitative agreement is observed with regard to the formation of secondary flows, migration of streamwise vortices, and distortion of the primary flow. Additional experimental data is needed to provide a basis for detailed quantitative evaluation of the analysis and flow predictions.

INTRODUCTION

A continuing problem in the design of inlets for airbreathing propulsion systems is the design of efficient subsonic diffusers. In the case of three-dimensional inlet diffusers, the cross-sectional shape of the ducting varies in the axial direction and it is frequently necessary to introduce offset bends (curved duct centerlines). The complicated diffuser geometry and the offset bends introduce strong secondary flows which have important effects on both diffuser performance and engine/inlet compatibility. A generalized subsonic diffuser analysis capable of being used as a design tool must account for several physical phenomena which frequently occur in practical diffusers. First, the analysis must be capable of treating the case when the wall boundary layers are turbulent and when the thickness is comparable to the local duct radius. Secondly, the analysis must be capable of treating the strong secondary flows which are commonly encountered in three-dimensional diffusers.

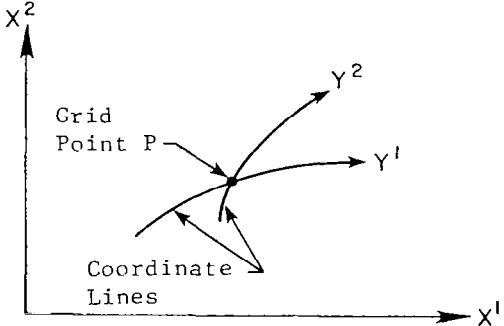
Although solution of the three-dimensional Navier-Stokes equations would be definitive, more cost effective approximate methods are proving attractive. One such approximate method has been developed by Briley and McDonald (Ref. 1) where a set of governing equations are developed by introducing approximations into the Navier-Stokes equations and then solved by spatial marching. This paper reports on a study to modify the analysis of Ref. 1 for use in constructed coordinate systems which may be nonorthogonal. By a judicious choice of dependent variables and of forms of the equations, some of the smoothness requirements for the coordinate system have been relaxed.

ANALYSIS

Coordinate Systems

A coordinate system is more than merely the grid points at which the governing equations are written. The coordinate system manifests itself as the geometric terms in the governing equations as is related to resolution of the physical processes and various length scales within the problem being studied. Although it is easy to overlook the part that the coordinate system plays in the governing equations, the requirements for a "good" coordinate system are found by finding the role these geometric terms play in the fluid dynamic equations. Different forms of the Navier-Stokes equations can impose different requirements for a coordinate system. For illustrative purposes a viscous term from two forms of the two-dimensional Navier-Stokes equations will be used.

First consider a point P in reference Cartesian coordinates (x^1, x^2) . The generalized coordinate lines are y^1 and y^2 passing through P and the Cartesian velocities are u^1 and u^2 . Using the quasi-linear form of the Navier-Stokes equations and Cartesian velocity components one of the viscous terms in the x^1 momentum equation would be

$$\frac{J}{Re} \frac{\partial Y^2}{\partial X^2} \frac{\partial}{\partial Y^2} \left(\mu \frac{\partial Y^2}{\partial X^2} \frac{\partial u^1}{\partial Y^2} \right) \quad (1)$$


where J is the Jacobian of the transformation from x^i into y^i and $\partial y^2 / \partial x^2$ is a component of the inverse transformation tensor. The Jacobian as well as the elements of the inverse transformation tensor are all related to the gradient of the position vector at the computational grid points relative to a fixed, reference Cartesian coordinate system.

Before continuing, let us identify this term in familiar Cartesian coordinates. In this case $J=1$, $\partial y^2/\partial x^2=1$, $y^2=x^2$ and $u^1=U$. By performing these simplifications we get:

$$\frac{1}{Re} \cdot 1 \cdot \frac{\partial}{\partial Y} \left(\mu \cdot 1 \cdot \frac{\partial u}{\partial Y} \right)$$

or

$$\frac{1}{Re} \frac{\partial}{\partial Y} \left(\mu \frac{\partial u}{\partial Y} \right) \quad (2)$$

which is the familiar form of the dominant viscous term in the Cartesian x momentum equation. From the simplicity of (2) one could easily forget the complexity of the term when expressed in general nonorthogonal form; but the complexity is real and the geometric terms are present and must be properly treated.

Returning to (1) it can be seen that the mathematical requirements on the inverse transformation tensor are the same as those on the fluids variables. That is, each element of (1) must be continuous, have continuous derivatives and be well defined by the computational grid points being used to solve the problem. Since the geometric terms in (1) are directly related to first derivatives of the locations of the computational grid points and these are in turn differentiated, the requirement on both the geometry and the velocity field is that in going from one grid point to another the second derivatives must be continuous and well defined. In addition, if the discretization of the differential equations into the difference equations is to be accurate, the geometric derivatives must not be large compared to the fluid dynamic terms.

As a second example, a corresponding viscous term is now examined in the general orthogonal form of the Navier-Stokes equations. For coordinate lines y^1 and y^2 and for velocity components along the coordinate directions u_1 and u_2 this viscous terms is

$$\frac{1}{Re h_1 h_2} \frac{\partial}{\partial Y^2} \left(\frac{h_1^2 \mu}{h_2} \frac{\partial \frac{u_1}{h_1}}{\partial Y^2} \right) \quad (3a)$$

where h_1 and h_2 are the metrics (e.g.)

$$h_1 = \left(\left(\frac{\partial x^1}{\partial Y^1} \right)^2 + \left(\frac{\partial x^2}{\partial Y^1} \right)^2 \right)^{1/2} \quad (3b)$$

To verify that this viscous term corresponds to the term examined in (1) for the case of Cartesian coordinates the metrics are all set to unity, $u_1=U$, $x^1=y^1$, $x^2=y^2$:

$$\frac{1}{Re} \frac{\partial}{\partial Y^2} \left(\mu \frac{\partial u}{\partial Y^2} \right) \quad (4)$$

which corresponds to (2).

Examination of (3a) shows that there is a second derivative of h_1 implying that h_1 must be continuous and have continuous derivatives. Equation (3b) shows that h_1 is itself a first derivative of the coordinate system. Thus, the requirement on the coordinate system for general orthogonal systems is that the coordinates must have continuous and well defined third derivatives.

In constructing coordinate systems one of the constraints is the required smoothness. One measure of the required smoothness is the order of continuous derivatives required. The above example demonstrates that the form of the governing equations can directly influence the adequacy of the coordinate system. This observation played a major role in both the selection of the forms of the governing equations and in the modifications made to the analysis of Ref. 1, which will now be discussed.

Governing Equations

The equations used in this analysis are based on the steady compressible Navier-Stokes equations. Three basic assumptions are made to permit a forward marching solution of the subsonic flow problem. First, the flow can be analyzed as being a primary flow with a transverse secondary flow. This primary flow is assumed to be approximately aligned with one of the coordinate directions. Second, the pressure field can be represented by a three-dimensional a priori known pressure field, such as comes from a three-dimensional potential flow analysis, plus a one-dimensional correction for viscous blockage effects and pressure loss.

$$P = P_{3-D}(x^1, x^2, x^3) + P_{1-D}(x^3) \quad (5)$$

The three-dimensional pressure field contains elliptic information about the flow (upstream influence). Third, the assumption of negligible second derivatives in the marching direction is also required to create an initial boundary value problem which can be solved by forward marching in one of the coordinate directions.

With these assumptions the Navier-Stokes equations are written using Cartesian velocities, u_i , and Cartesian coordinates, x^i . Although subsequent forms of these equations are to be evaluated in general nonorthogonal coordinates, y^i , the use of

Cartesian velocities and Cartesian directions for the vector equations will result in the favorable smoothness properties discussed above. The Cartesian coordinate system x^i , is rotated at each computational step to keep the x^3 Cartesian direction aligned with the tangent to the duct centerline ensuring that even when the duct contains large bends, the x^3 coordinate direction is always roughly aligned with the primary flow direction. The x^1 coordinate direction is aligned with the outward facing normal. Special treatment of cases where the centerline curvature is zero is readily provided. The vector quantities, velocity and vorticity, are also transformed to stay consistent with the Cartesian directions.

The velocity vector, V , is decomposed into a primary flow component, u_3 , normal to the cross plane and a secondary flow component. The secondary flow is further decomposed into parts associated with the irrotational cross flow, \bar{V}_ϕ , and the rotational cross flow, \bar{V}_ψ :

$$\bar{V} = \bar{u}_3 + \bar{V}_s \quad (6)$$

$$\bar{V} = \bar{u}_3 + \bar{V}_\phi + \bar{V}_\psi \quad (7)$$

where

$$\nabla_s \times (\bar{V}_\phi) = 0 \quad (8)$$

$$\nabla_s \cdot (\rho \bar{V}_\psi) = 0 \quad (9)$$

and ∇_s is the surface gradient operator in the cross plane:

$$\nabla_s = \frac{\partial}{\partial x^1} \bar{i} + \frac{\partial}{\partial x^2} \bar{j} = \frac{\partial Y^n}{\partial X^1} \frac{\partial}{\partial Y^n} \bar{i} + \frac{\partial Y^n}{\partial X^2} \frac{\partial}{\partial Y^n} \bar{j} \quad (10)$$

for $n=1,2$.

Since the x^3 direction is the primary flow direction, the x^3 momentum equation in Cartesian coordinates is

$$\begin{aligned} \rho u_j \frac{\partial u_3}{\partial x^j} = & - \frac{\partial P_{3-D}}{\partial x^3} - \frac{\partial P_{1-D}}{\partial x^3} + F_3 \\ & + \frac{\partial}{\partial x^j} \left[\mu_e \left((1 - \delta_{j3}) \left(\frac{\partial u_3}{\partial x^j} + \frac{\partial u_j}{\partial x^3} \right) - \frac{2}{3} \delta_{3j} (1 - \delta_{k3}) \frac{\partial u_k}{\partial x^k} \right) \right] \end{aligned} \quad (11)$$

where F_3 is the body force in the x^3 direction and μ_e is the effective viscosity. Using the nonorthogonal computational coordinates, y^i , the x^3 momentum equation:

$$\begin{aligned} \rho u_j \frac{\partial y^i}{\partial x^j} \frac{\partial u_3}{\partial y^i} = & - \frac{\partial y^i}{\partial x^3} \frac{\partial P_{3-D}}{\partial y^i} - \frac{\partial y^3}{\partial x^3} \frac{\partial P_{1-D}}{\partial y^3} + F_3 \\ & + \frac{\partial y^i}{\partial x^j} \frac{\partial}{\partial y^i} \left[\mu_e \left((1 - \delta_{j3}) \left(\frac{\partial y^n}{\partial x^j} \frac{\partial u_3}{\partial y^n} + \frac{\partial y^n}{\partial x^3} \frac{\partial u_j}{\partial y^n} \right) \right. \right. \\ & \left. \left. - \frac{2}{3} \delta_{3j} (1 - \delta_{k3}) \frac{\partial y^n}{\partial x^k} \frac{\partial u_k}{\partial y^n} \right) \right] \end{aligned} \quad (12)$$

is solved along with the global mass flux conservation relation

$$\iint \frac{\partial \rho u_3}{\partial x^3} dx^1 dx^2 = 0 \quad (13)$$

the energy equation:

$$h_0 = \text{const.} \quad (14)$$

and the equation of state:

$$P = P_{3-D} + P_{1-D} = \rho RT \quad (15)$$

to determine u_3 , ρ , and $P_{1-D}(x^3)$.

The continuity equation is written as:

$$\nabla \cdot (\rho \bar{V}) = \frac{\partial u_3 \rho}{\partial x^3} + \nabla_s \cdot (\rho \bar{V} \phi) = 0 \quad (16)$$

Introducing a potential function ϕ :

$$\nabla_s \cdot (\rho \nabla_s \phi) = - \frac{\partial u_3 \rho}{\partial x^3} \quad (17)$$

this Poisson equation is solved in the form:

$$\frac{\partial y^j}{\partial x^i} \frac{\partial}{\partial y^j} \left(\rho \frac{\partial y^k}{\partial x^i} \right) \frac{\partial \phi}{\partial y^k} + \rho \left(\frac{\partial y^k}{\partial x^i} \right)^2 \frac{\partial^2 \phi}{\partial y^k{}^2} \quad (18)$$

$$+ 2\rho \frac{\partial y^l}{\partial x^i} \frac{\partial y^2}{\partial x^i} \frac{\partial^2 \phi}{\partial y^l \partial y^2} = - \frac{\partial y^n}{\partial x^3} \frac{\partial \rho u_3}{\partial y^n}$$

for $k=1,2$ where ϕ is defined by:

$$\nabla_s \phi = \bar{v}_\phi \quad (19)$$

and satisfies (8).

The remaining unknown is the rotational cross flow velocity component, \bar{v}_ψ . This is found by cross differentiating and combining x^1 and x^2 momentum equations to form the vorticity transport equation in the x^3 direction. One form of this equation is:

$$\begin{aligned} u_j \frac{\partial \Omega_3}{\partial x^j} - \Omega_j \frac{\partial u_3}{\partial x^j} - u_j \frac{\partial \rho}{\partial x^j} \frac{\Omega_3}{\rho} &= \frac{\mu_e}{\rho} \frac{\partial^2 \Omega_3}{\partial x^{j^2}} + \frac{\partial(F_1/\rho)}{\partial x^2} - \frac{\partial(F_2/\rho)}{\partial x^1} \\ &+ \frac{1}{\rho} \left(\frac{\partial \mu_e}{\partial x^2} - \frac{\partial \mu_e}{\partial x^1} \right) \frac{\partial}{\partial x^1} \left((1 - \delta_{3j}) \left(\frac{\partial u_1}{\partial x^j} - \frac{\partial u_2}{\partial x^j} \right) + \frac{\partial u_j}{\partial x^1} - \frac{\partial u_j}{\partial x^2} - \frac{2}{3} (\delta_{1j} - \delta_{2j}) \frac{\partial u_k}{\partial x^k} \right) \\ &+ \frac{1}{\rho} \frac{\partial \mu_e}{\partial x^j} \left(\frac{\partial}{\partial x^2} \left(\frac{\partial u_1}{\partial x^j} - \frac{2}{3} \delta_{1j} \frac{\partial u_k}{\partial x^k} \right) - \frac{\partial}{\partial x^1} \left(\frac{\partial u_2}{\partial x^j} - \frac{2}{3} \delta_{2j} \frac{\partial u_k}{\partial x^k} \right) \right) \quad (20) \\ &+ \frac{1}{\rho} \frac{\partial^2 \mu_e}{\partial x^2 \partial x^j} \left(\frac{\partial u_1}{\partial x^j} + \frac{\partial u_j}{\partial x^1} - \frac{2}{3} \delta_{1j} \frac{\partial u_k}{\partial x^k} \right) \\ &+ \frac{1}{\rho} \frac{\partial^2 \mu_e}{\partial x^1 \partial x^j} \left(\frac{\partial u_2}{\partial x^j} + \frac{\partial u_j}{\partial x^2} - \frac{2}{3} \delta_{2j} \frac{\partial u_k}{\partial x^k} \right) \\ &+ \frac{1}{\rho^2} \left(\frac{\partial \rho}{\partial x^2} \frac{\partial P_{3-D}}{\partial x^1} - \frac{\partial \rho}{\partial x^1} \frac{\partial P_{3-D}}{\partial x^2} \right) \end{aligned}$$

where u_1 and u_2 are components of

$$u_1 \bar{i} + u_2 \bar{j} = \bar{v}_s = \bar{v}_\phi + \bar{v}_\psi \quad (21)$$

and the vorticity is defined as:

$$\Omega_1 = \frac{\partial u_2}{\partial x^3} - \frac{\partial u_3}{\partial x^2} \quad (22)$$

$$\Omega_2 = \frac{\partial u_3}{\partial x^1} - \frac{\partial u_1}{\partial x^3} \quad (23)$$

$$\Omega_3 = \frac{\partial u_1}{\partial x^2} - \frac{\partial u_2}{\partial x^1} \quad (24)$$

To solve this equation for \bar{v}_ψ a stream function, $\bar{\psi}$ in the x^3 direction, is introduced satisfying:

$$\nabla_s \times \bar{\psi} = \rho \bar{v}_\psi \quad (25)$$

Using (24) the stream function and the nominally streamwise component of vorticity, Ω_3 , are related by

$$\begin{aligned} \Omega_3 &= \nabla_s \times \bar{v}_s \\ &= \nabla_s \times (\bar{v}_\phi + \bar{v}_\psi) \\ &= \nabla_s \times \bar{v}_\psi \\ \Omega_3 &= \nabla_s \times \left(\frac{1}{\rho} \nabla_s \times \bar{\psi} \right) \end{aligned} \quad (26)$$

Equations (20) and (26) are solved simultaneously for $\bar{\psi}$ and Ω_3 . Since the remaining parameters are either known functions or expressible in terms of known functions, Ω_3 and $\bar{\psi}$.

Flow in Ducts with Superelliptic Cross Sections

The analysis of the previous section was applied to the flow in a general class of subsonic diffuser ducts. The duct centerline is defined by polynomials and the cross sections are described by superellipses in a plane locally normal to the centerline. The duct boundaries are coordinate surfaces, greatly simplifying the boundary conditions. This coordinate system is described in detail in Ref. 2. Note that the grid distribution functions of Ref. 2 have been replaced. For radial distributions to resolve the boundary layer:

$$R = \frac{\tanh(Dr)}{\tanh(D)} \quad (27)$$

where R is physical radius, r is the radial computational coordinate parameter and D, the damping function which determines the severity of the distribution, is controlled through the parameter α by:

$$D = \frac{2}{1-\alpha} \quad (28)$$

A circumferential distribution function is also used to cluster grid points into regions of tight wall curvatures. The equally spaced computational coordinate t is related to the physical angle Θ in a quadrant by the relation:

$$\begin{aligned} \Theta &= A \sinh \left(\frac{D(t-c)}{t_2 - t_1} \right) + B \\ t_1 &= 0, \quad t_2 = 1 \\ \Theta_1 &= 0 \quad \Theta_2 = \pi/2 \\ \Theta_c &= \tan^{-1}(S^2) \\ S &= \text{shape (ratio of major to minor axis)} \\ E &= \text{superelliptic exponent} \\ R &= \frac{\Theta_1 - \Theta_c}{\Theta_2 - \Theta_c}, \quad D = \ln(2 * E + 2 * S) \\ DZM &= \frac{\ln(2 * E + 2 * S)}{t_2 - t_1} \end{aligned} \quad (29)$$

where:

$$C = \frac{1}{DZM} \tanh^{-1} \left[\frac{\sinh(DZM \cdot t_1) - R \cdot \sinh(DZM \cdot t_2)}{\cosh(DZM \cdot t_1) - R \cdot \cosh(DZM \cdot t_2)} \right] \quad (30)$$

$$B = \Theta_1 + \frac{\Theta_2 - \Theta_1}{1 - \frac{\sinh(DZM \cdot (t_2 - C))}{\sinh(DZM \cdot (t_1 - C))}} \quad (31)$$

$$A = \frac{\Theta_2 - \Theta_1}{\sinh(DZM(t_2 - C)) - \sinh(DZM(t_1 - C))} \quad (32)$$

This distribution function, (29), clusters grid points toward $\Theta = \Theta_c$. Several examples of the effects of (27) and (29) are presented in Fig. 1 for a series of cross sectional shapes.

The governing equations used in this application are:
MOMENTUM in the X^3 direction

$$\begin{aligned} \rho u_j \frac{\partial \gamma^j}{\partial x^j} \frac{\partial u_3}{\partial \gamma^i} = & - \frac{\partial \gamma^i}{\partial x^3} \frac{\partial P_{3-D}}{\partial \gamma^i} - \frac{\partial \gamma^3}{\partial x^3} \frac{\partial P_{1-D}}{\partial \gamma^3} \\ & + \frac{\partial \gamma^i}{\partial x^j} \frac{\partial}{\partial \gamma^i} \left[\mu_e \left((1 - \delta_{j3}) \left(\frac{\partial \gamma^n}{\partial x^j} \frac{\partial u_3}{\partial \gamma^n} + \frac{\partial \gamma^n}{\partial x^3} \frac{\partial u_j}{\partial \gamma^n} \right) \right. \right. \\ & \left. \left. - \frac{2}{3} \delta_{3j} (1 - \delta_{k3}) \frac{\partial \gamma^n}{\partial x^k} \frac{\partial u_k}{\partial \gamma^n} \right) \right] \end{aligned} \quad (33)$$

from CONTINUITY

$$\begin{aligned} \frac{\partial \gamma^j}{\partial x^i} \frac{\partial}{\partial \gamma^j} \left(\rho \frac{\partial \gamma^k}{\partial x^i} \right) \frac{\partial \phi}{\partial \gamma^k} + \rho \left(\frac{\partial \gamma^k}{\partial x^i} \right)^2 \frac{\partial^2 \phi}{\partial \gamma^{k^2}} \\ + 2\rho \frac{\partial \gamma^i}{\partial x^i} \frac{\partial \gamma^2}{\partial x^i} \frac{\partial^2 \phi}{\partial \gamma^i \partial \gamma^2} = - \frac{\partial \gamma^n}{\partial x^3} \frac{\partial \rho u_3}{\partial \gamma^n} \end{aligned} \quad (34)$$

VORTICITY TRANSPORT in the X^3 direction

$$u_j \frac{\partial \Omega_3}{\partial x^j} - \Omega_j \frac{\partial u_3}{\partial x^j} = \frac{\mu_e}{\rho} \frac{\partial^2 \Omega_3}{\partial x^{j^2}} \quad (35)$$

STREAM FUNCTION

$$\begin{aligned} \frac{\partial \gamma^j}{\partial x^i} \frac{\partial}{\partial \gamma^j} \left(\frac{1}{\rho} \frac{\partial \gamma^k}{\partial x^i} \right) \frac{\partial \psi}{\partial \gamma^k} + \frac{1}{\rho} \left(\frac{\partial \gamma^k}{\partial x^i} \right)^2 \frac{\partial^2 \psi}{\partial \gamma^{k^2}} \\ + \frac{2}{\rho} \frac{\partial \gamma^i}{\partial x^i} \frac{\partial \gamma^2}{\partial x^i} \frac{\partial^2 \psi}{\partial \gamma^i \partial \gamma^2} = - \Omega_3 \end{aligned} \quad (36)$$

The vorticity transport equation was used in simplified form for convenience during the development phase of this study. Use of equation (20) for vorticity transport is anticipated.

At each marching step the computational domain has two symmetry boundaries, a boundary which is the duct wall and a boundary which is a small tube surrounding the centerline singularity (see Fi. 2). The boundary conditions for the X^3 momentum equation are $\partial u / \partial n = 0$ on the two symmetry surfaces where n is the local surface normal, $u = 0$ on the wall and

$$u \frac{du}{dX^3} = - \frac{1}{\rho} \frac{dP}{dX^3}$$

at the centerline.

The scalar potential equation for ϕ has the boundary condition $\phi=0$ on all boundaries.

The vorticity and stream function equations are solved sequentially and coupled iteratively. The stream function boundary condition $\psi=0$ is applied at all boundaries. The vorticity boundary condition $\Omega_3=0$ is applied along the symmetry and centerline boundaries. On the wall the vorticity boundary condition is derived following Briley & McDonald (Ref. 1), by writing the stream function equation (36) on the wall using central difference formulas. The additional constraint needed to eliminate the added variable is the no-slip condition for the cross flow. These equations are

$$\begin{aligned} & \frac{\partial Y^j}{\partial X^i} \frac{\partial}{\partial Y^j} \left(\frac{1}{\rho} \frac{\partial Y^2}{\partial X^i} \right) \frac{\partial \psi}{\partial Y^2} + \frac{1}{\rho} \left(\frac{\partial Y^2}{\partial X^i} \right)^2 \frac{\partial^2 \psi}{\partial Y^2{}^2} \\ & + \frac{2}{\rho} \frac{\partial Y^1}{\partial X^i} \frac{\partial Y^2}{\partial X^i} \frac{\partial^2 \psi}{\partial Y^1 \partial Y^2} = - \Omega_3 \end{aligned} \quad (37)$$

and setting the slip velocity from the solution of the stream function-vorticity equations equal and opposite to the slip velocity from the solution of the scalar potential equation yields:

$$\frac{\partial \psi}{\partial Y^2} = \rho \frac{\frac{\partial Y^1}{\partial X^1} V_\phi + \frac{\partial Y^1}{\partial X^2} W_\phi}{\frac{\partial Y^1}{\partial X^2} \frac{\partial Y^2}{\partial X^1} - \frac{\partial Y^1}{\partial X^1} \frac{\partial Y^2}{\partial X^2}} \quad (38)$$

where

$$v_{\phi} = \frac{\partial Y^2}{\partial X^1} \frac{\partial \phi}{\partial Y^2} \quad w_{\phi} = \frac{\partial Y^2}{\partial X^2} \frac{\partial \phi}{\partial Y^2}$$

on the wall.

The mixing length model used in this analysis employs the eddy-viscosity formulation for the Reynolds stresses, i.e.,

$$\rho \overline{v^i v^j} = - \frac{\mu_T}{Re} \frac{\partial v^j}{\partial x_i} \quad (39)$$

Hence, this formulation still suffers from the physical shortcoming that there is zero Reynolds stress wherever the velocity gradient is zero. In addition, the eddy viscosity formulation is isotropic which may be incorrect in many three-dimensional and swirling flows. However, for practical calculations of turbulent internal flows there are as yet no other transport models which are either suitable or as relatively well developed.

The mixing length turbulence model employed in this analysis is based on a mixing length distribution. The mathematical form of the expression for the turbulent viscosity follows from Ref. 3:

$$\frac{\mu_T}{Re} = \rho \ell^2 (2\bar{\bar{e}}:\bar{\bar{e}})^{1/2} \quad (40a)$$

where $\bar{\bar{e}}$ is the mean flow rate of strain tensor

$$\bar{\bar{e}} = 1/2 [(\nabla \vec{v}) + (\nabla \vec{v})^T] \quad (40b)$$

The mixing length ℓ is determined from the Buleev formula (Ref. 4)

$$\frac{1}{\ell} = \frac{1}{2\kappa} \int_0^{2\pi} \frac{1}{S} d\theta \quad (41)$$

where κ is the von Karman constant and S and θ are defined in Fig. 3.

Potential Flow

The present application of the analysis presented in the previous section uses a three-dimensional potential flow to supply the a priori known pressure field used in the viscous flow analysis. The potential flow is computed in the computational coordinate system by solving the equation

$$\nabla^2 \phi = 0 \quad (42)$$

$$\frac{\partial^2 \phi}{\partial X^1{}^2} + \frac{\partial^2 \phi}{\partial X^2{}^2} + \frac{\partial^2 \phi}{\partial X^3{}^2} = 0 \quad (43)$$

or expressed in the computational coordinate system:

$$\begin{aligned}
& \frac{\partial \gamma^i}{\partial x^1} \frac{\partial}{\partial \gamma^i} \left(\frac{\partial \gamma^j}{\partial x^1} \frac{\partial \phi}{\partial \gamma^j} \right) + \frac{\partial \gamma^i}{\partial x^2} \frac{\partial}{\partial \gamma^i} \left(\frac{\partial \gamma^j}{\partial x^2} \frac{\partial \phi}{\partial \gamma^j} \right) \\
& + \frac{\partial \gamma^i}{\partial x^3} \frac{\partial}{\partial \gamma^i} \left(\frac{\partial \gamma^j}{\partial x^3} \frac{\partial \phi}{\partial \gamma^j} \right) = 0
\end{aligned}
\tag{44}$$

where ϕ is the velocity potential, x^i are the Cartesian coordinates and γ^i are the computational coordinates. This equation is solved using an iterative scalar ADI procedure. The boundary conditions at the duct wall is that there is no flow through the wall, i.e. $\frac{\partial \phi}{\partial n} = 0$. Since the potential, ϕ , is dimensionless the inflow and outflow values are set to 0 and 1 respectively. The duct centerline would represent a coordinate singularity so the coordinate system used extends from the duct walls down to a small tube of finite radius around the centerline. The boundary condition applied at the centerline is derived from a zero velocity normal to the symmetry plane and permitting a velocity component tangent to the symmetry plane. Since the solution technique is iterative, the velocity boundary condition is lagged and updated every few iterations. The area in the tube around the centerline is small and this explicit, rather than implicit, handling of the boundary condition appears to have little if any adverse influence on the observed convergence properties of the solution procedure for solving Eq. (44).

Once the converged value of the potential, ϕ , is found, the non-dimensional velocities at each grid point are computed. These velocities are scaled to be compatible with the specified reference conditions. From the velocities the corresponding pressure field is computed and values of pressure coefficient are computed and saved on permanent storage for later use in the viscous spatial marching calculations.

Calculations

The above analysis was applied to a series of test problems. The first case presented here is the flow in the entrance region of a straight circular pipe. The calculations were compared to the experimental data of Reshotko (Ref. 5). The excellent agreement with the data is shown in Fig. 4.

The second case was of turbulent flow through a circular pipe undergoing an S-shaped bend. The bend was offset 1 diameter in a streamwise distance of 5 diameters (Fig. 5). The entrance Mach number was 0.2 and the entrance Reynolds number was 10^6 . Although no test data was available to quantitatively evaluate the results, the test case was apparently successful. A qualitative evaluation has been made by comparing salient features of the computed flow with the flow measured in a model of the Boeing 727 Center Duct Inlet (Ref. 6). It must be emphasized that the computed case was for different geometry, Reynolds number and Mach number than the tested case. However, not only are the classical secondary flow patterns clearly discernible in both cases, but the development of the secondary flow patterns appears to occur in the same manner. The locations marked A, B, C and D refer to cross sections where comparisons will be presented. Sections A are near the center of the first bend, sections B are just after the inflection, sections C are just after the center of the second bend, and sections D are at the ends of the ducts. Figure 6 presents the contours of total pressure at the bottom of the 727 duct for stations A, B and C. The growing region of low total pressure is clearly seen. Also shown are contours of streamwise velocity at the bottom of the computed S-shaped duct. In the case presented these streamwise velocity contours have nearly the same shape as total pressure contours. Here again the growing region of low total pressure is clearly seen at the bottom of the duct. A comparison of sections D in Figure 7 shows the classical total pressure contour shapes for S-shaped bends. Figure 8 also shows these classical exit plane total pressure contours from three other S-shaped bends (Ref. 7).

SUMMARY AND CONCLUSIONS

An analysis is presented for computing three-dimensional subsonic flow in diffusers. Following Briley and McDonald, approximations are introduced into the Navier-Stokes equations to produce a system of equations which can be solved by forward marching. This paper reports on a study to adapt the above analysis for use with nonorthogonal constructed coordinate systems.

At each computational plane a local Cartesian coordinate system is defined at the duct centerline with one coordinate direction tangent to the centerline and another coordinate direction aligned with the outward facing normal. Special treatment of cases where the centerline curvature is zero is readily provided. Velocity components are defined to be aligned with these Cartesian directions and those governing equations that are vector equations are written in these local Cartesian directions. At each marching station the vector quantities computed at the previous station are transformed into these new vector directions.

The resulting partial differential equations are transformed into the constructed coordinate system. These equations contain only first derivatives of the elements of the transformation from Cartesian to constructed coordinates as contrasted with the familiar general orthogonal equations which contain second derivatives of the metric scale factors (h 's). This reduced sensitivity of the governing equations to the details of the coordinate system permits more flexibility in the coordinate construction process. A family of duct shapes with superelliptic cross sections is currently available within the code representing a large class of diffuser shapes. These coordinates are nonorthogonal. The analysis developed in this study is applicable to more general cross-sectional shapes than are currently available within the code.

The above analysis was applied to subsonic viscous flow in several ducts. Qualitative agreement with experimental measurements was encouraging since the formation and migration of the vortex seen in the measurements was also present in the computed results. Additional experimental data is needed to provide a basis for detailed quantitative evaluation of the analysis.

The current version of the computer code solves the streamwise vorticity and stream function equations by coupling them through a sequential iterative procedure. A preferred method would be to solve these equations as an implicitly coupled block system. This is expected to improve convergence properties of these equations and permit larger streamwise steps to be taken.

REFERENCES

1. Briley, W. R. and McDonald, H.: Analysis and Computation of Viscous Subsonic Primary and Secondary Flows, AIAA Paper No. 79-1453.
2. Eiseman, P. R., McDonald, H. and Briley, W. R.: Method for Computing Three-Dimensional Viscous Diffuser Flows. United Technologies Research Center Report R75-911737-1, July 1975.
3. Beer, J. M. and Chigier, N. A.: Combustion Aerodynamics. Wiley, New York, 1972.
4. Buleev, N. I.: Theoretical Model of the Mechanisms of Turbulent Exchange in Fluid Flow. Atomic Energy Research Establishment (U.K.) Translation 957, 1963.
5. Reshotko, E.: Experimental Study of the Stability of Pipe Flow, Pt. 1, Establishment of an Axially Symmetric Poiseuille Flow. Jet Propulsion Laboratory Progress Report No. 20-364, October 1958.
6. Kaldschmidt, G., Syltebo, B. E., and Ting, C. T.: "Design and Results of Low Speed Performance Confirmation Model Test of a 727 Airplane Center Duct Inlet for Refanned JT8D Engines:", The Boeing Company, 1974.
7. Bansod, P. and Bradshaw, P.: "The Flow in S-shaped Ducts", The Aeronautical Quarterly, Vol. XXIII, Part 2, May 1972.

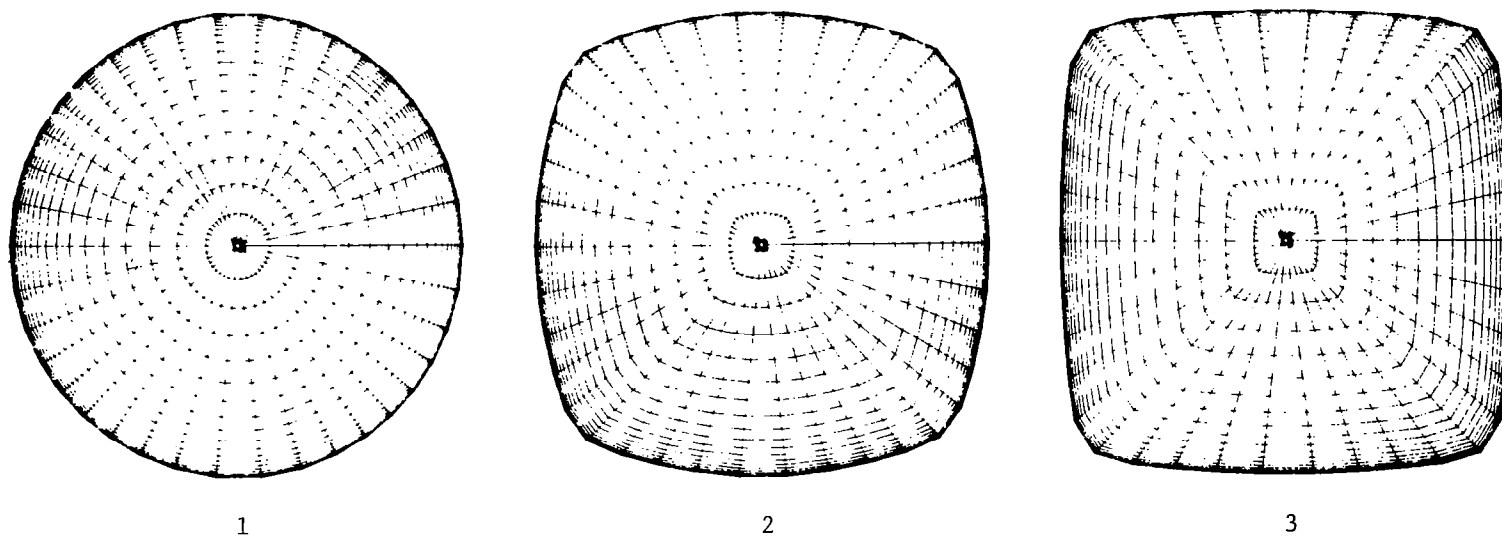


Fig. 1a - Variation in Superelliptic Exponent (Shape=1).

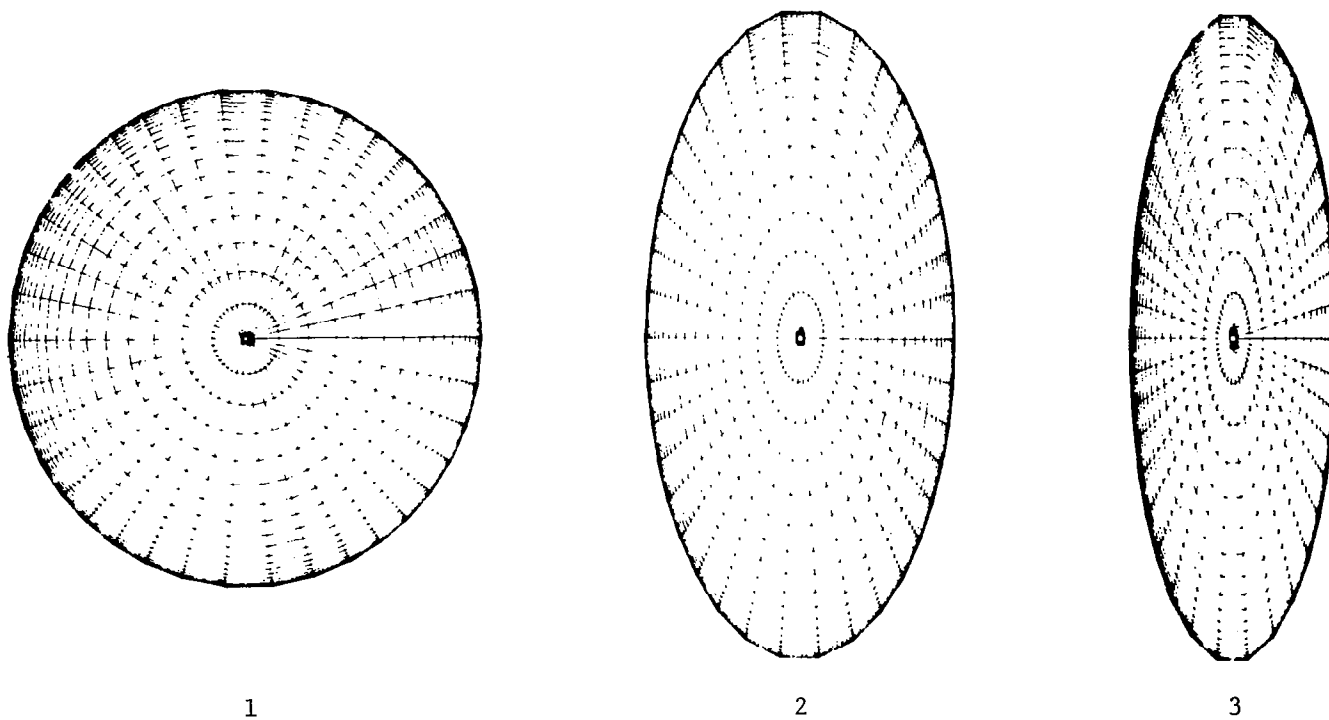


Fig. 1b - Variation in Shape (Exponent=2).

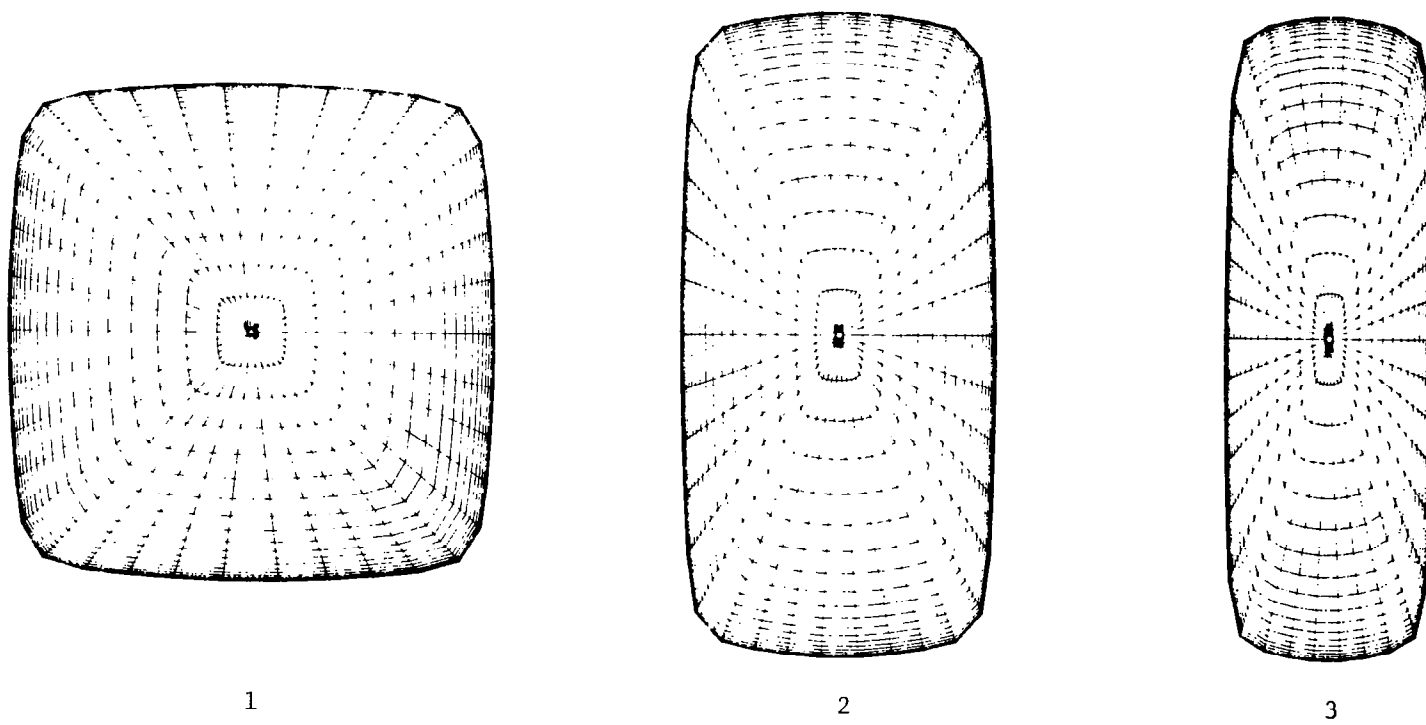


Fig. 1c - Variation in Shape (Exponent=5).

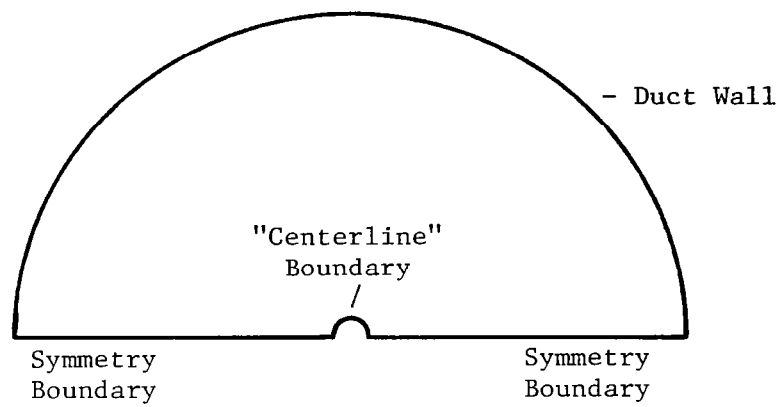


Fig. 2 - Computational Domain.

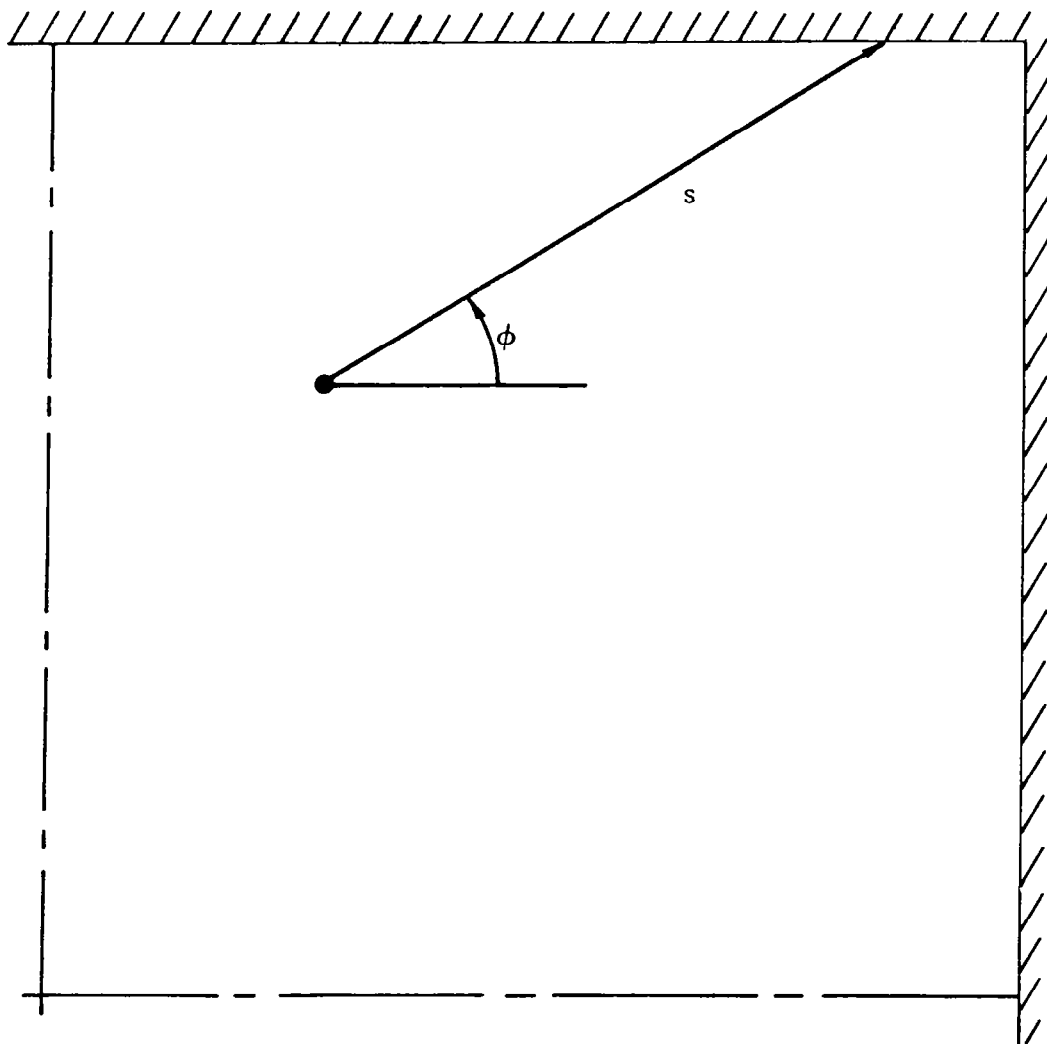


Fig. 3 - Notation for Calculating Buleev Length Scale.

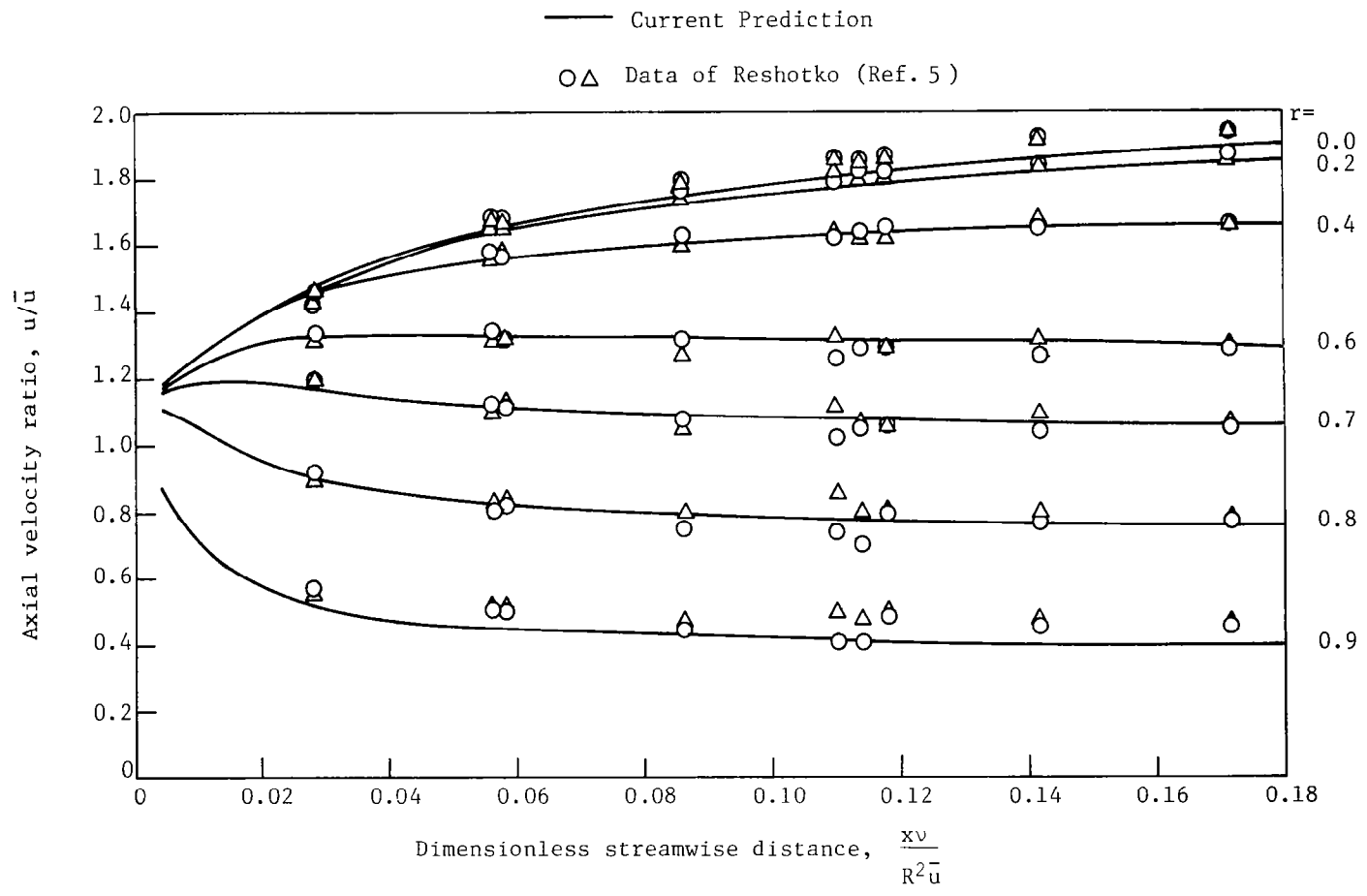


Figure 4 . - Development of the velocity profile in a circular pipe

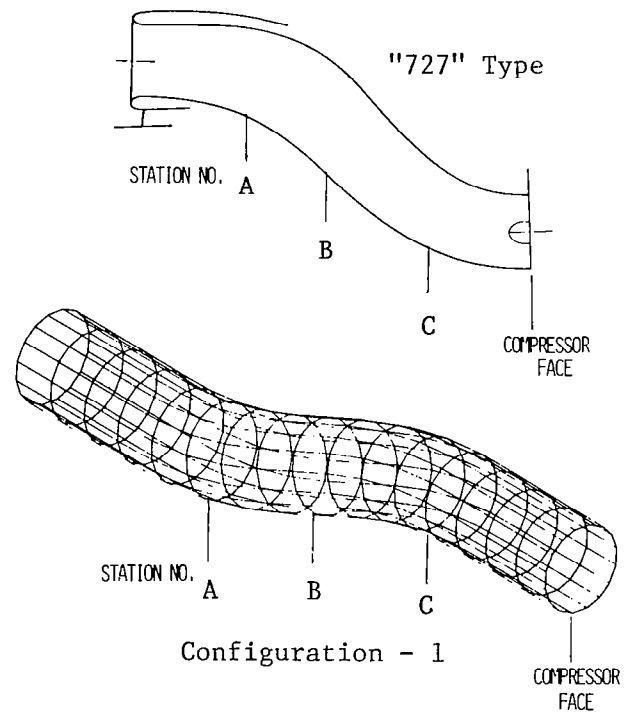


Fig. 5 - S-Duct Diffusers.

"727"
Total Pressure

Configuration - 1
Total Velocity

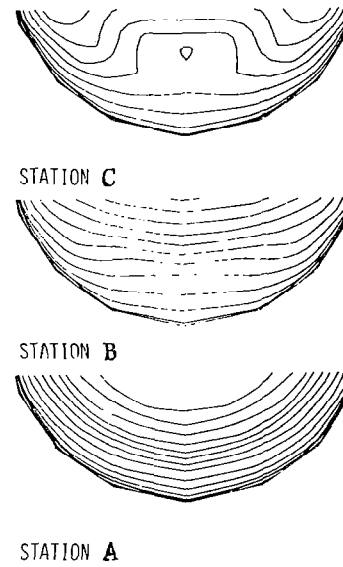
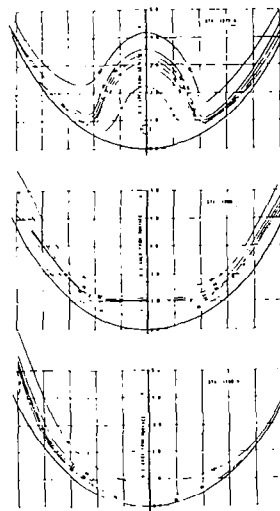


Fig. 6 - Development of Deficit Region in S-Duct Diffusers.

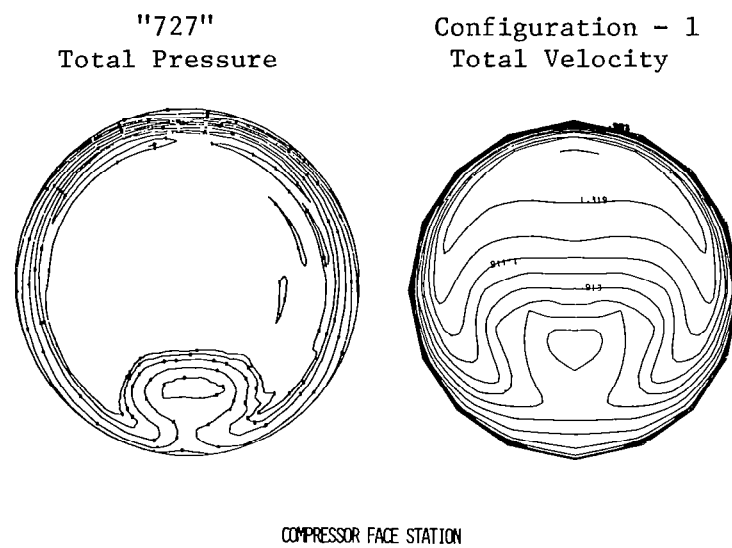


Fig. 7 - Compressor Face Profiles.

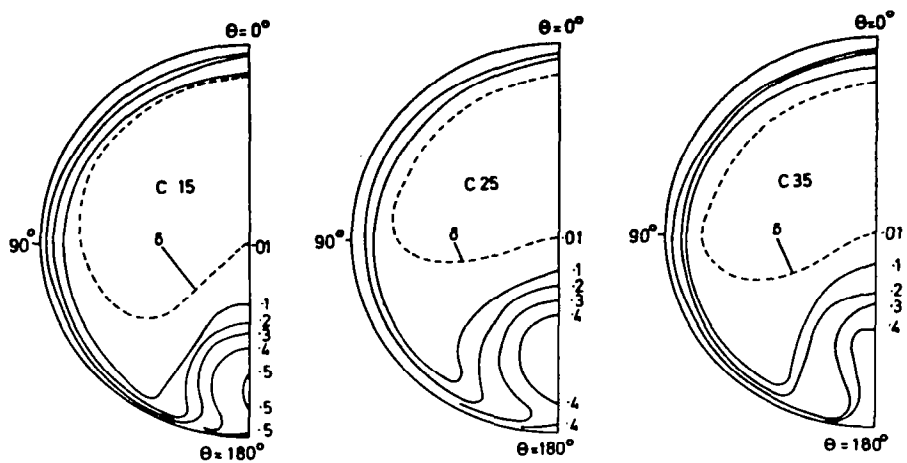


Figure 8. - Contours of total-pressure loss coefficient at exit, (Ref. 5).

SYMBOL TABLE

x	Cartesian coordinate
y^i	General curvilinear coordinate
$\bar{i}, \bar{j}, \bar{k}$	Cartesian unit vectors
δ_{ij}	Kroniker delta
\bar{V}	Velocity vector
U_i	Velocity component
P	Pressure
ρ	Density
Re	Reynolds number
μ	Viscosity
μ_e	Effective turbulent viscosity
Ω_i	Vorticity component
ϕ	Scalar potential function
ψ	Stream function
r	Radial computational coordinate parameter
t	Azimuthal computational coordinate parameter

APPENDIX
COMPUTER CODE INPUT AND OUTPUT

The PEPSIG code input is of the form:

MODE, TITLE

Namelist Data

.
.
.
.
.
.

MODE, TITLE

Namelist Data

.
.
.
.
.
.

MODE, TITLE

Namelist Data

.
.
.
.
.
.

STOP

The mode parameter selects which of the four functions available within the code are to be used.

MODE - 4 geometric preprocessing

3 geometry written for potential flow on logical unit #10

2 potential flow calculation

1 parabolized Navier-Stokes

When operating in MODE = 4, the code will solve a series of simultaneous equations to determine polynomials $Y = f(X)$ from tabulations of Y , Y' and/or Y'' versus X . The input is specified through NAMELIST:

\$L

NEQ - number of equations

XIN - input table of X values

YIN - input of Y , Y' or Y'' according to corresponding value of ID

ID - 0 YIN is Y

1 YIN is Y'

2 YIN is Y''

NX - number of locations in the interval X_1 , X_2 at which the resulting polynomial is to be evaluated.

X_1 , X_2 - interval in which the resulting polynomial is to be evaluated

The input for MODE = 3, 2 and 1 is provided through three Namelist tables. Although the code is still in the development stage and elegant input has not yet been devised, the Namelist method provides a serviceable means of setting up the cases to be run. The three Namelists are, in order of being read: GEOM, FLUIDS, and SWITCH. The numbers in parenthesis following the explanation of the input variable are the recommended values.

\$GEOM

NRAD - Number of grid points in the radial direction (21)

MTHETA - Number of grid points in the circumferential direction (21)

RTUBE - Radius of the tube put around the centerline to remove the geometric singularity (0.01)

P(1, J) - Coefficients of polynomial in x for shape factor - ratio of major to minor axis where:

$$S.F. = P(1,1) + P(1,2) x + P(1,3) x^2 + P(1,4) x^3 \dots + P(1,11) x^{10}$$

P(2, J) - Coefficients of polynomial in x for radius of major axis

P(4, J) - Coefficients of polynomial in x for superelliptic exponent between 2 and 10

PA(3,1,J)- Coefficients of polynomial in x for transverse Cartesian component of centerline curve. Set to zero for straight duct.

NOTE: The P and PA arrays determine the location of the grid points. Since the position vector of the grid points is differentiated twice within the code, the piecewise polynomials describing these locations must be continuous to two derivatives. Small values of higher derivatives is also recommended.

YZERO - Reference length in ft. (1.0)
 NS - Number of the last marching station to be computed
 NFIRST - Number of the first marching station whose geometry is to be specified (usually 1)
 X(NFIRST) - Nondimensionalized location of first marching step whose geometry is to be specified
 DX - Initial step size
 AP - Ratio of consecutive step sizes in the marching direction

$$x(i) = x(i-1) + AP * [x(i-1) - x(i-2)]$$

 IPA - Circumferential distribution function, 2 is equally spaced, 3 is automatic distribution, (3)
 VIS - α in Eq. (28) (.3)
 IPB - Radial distribution function 2 is equally spaced, 3 is packed toward the wall (3)
 IRSTIN - The station number to be read in for restart
 If IRSTIN = 0, not a restart case
 IRSTOT - The interval for saving restart information
 If IRSTOT = 0, no restart information saved
 JRSTIN - Logical file name from which restart information is to be read
 JRSTOT - Logical file name onto which restart information is to be written
 NFILE - The sequence number in JRSTIN of the desired restart information
 NSAVED - The number of restart stations saved on JRSTOT; must be initialized in inputs to the number of stations already written (and to be preserved) on JRSTOT. Nominally initialized NSAVED = 0.

NOTE: By setting JRSTOT = JRSTIN and NFILE = NSAVED, one file can be used for both read and write information, without destroying the already saved information.

\$FLUIDS

RZERO - Reference density in lbm/ft³
 UZERO - Reference velocity in ft/sec
 CMACH - Reference Mach Number

NOTE: Set either CMACH or UZERO and the other will be computed within the code.

REY - Reynolds number based on UZERO, YZERO and RZERO. Reference viscosity is determined by $VISCOS = UZERO*YZERO+RZERO/REY$

KTURB - 0 Laminar

- 1 Turbulent

YSLOT(2)- Initial nondimensionalized boundary layer thickness

\$\$SWITCH

NE1PF - Number of circumferential grid points used in potential flow

NE2PF - Number of radial grid points used in potential flow

IGDMP - 2 Dumps streamwise momentum equation coefficients loaded into matrix inverter

0 No dump

IPLOT - 1 Write plot file (logical unit #8)

0 No plot file

ICOEFG(1,N) - Auxiliary array which controls various options within the code.

In general a value of 0 means the option is off, a value of 1 means on.

N

1 COEFG convective terms printout

2 COEFG first viscous terms printout

3 COEFG second viscous terms printout

4 COEFG inviscid pressure gradient printout

5 COEFG viscous pressure gradient printout

6 PFIELD, CPI=0

7 PFLOW inter dump -1, full dump 1 or 2

8 EI dump from CROSEC

9 output PHI, PSI velocities

10 output PHI, PSI Cartesian velocities

11 output Cartesian velocities

12 ADI dump PSI

13 ADI dump vorticity

14 ADI dump PHI

- 15 input NAMELIST dump
- 16 IPRFSE dump
- 17 DYFA mixed der. diagnostic message
- 18 level 2 output
- 19 PFIELD drum reading information
- 20 output for ITER=1,2

ICOEF(2,N) N

- 1 wall vorticity for no slip (COEFVS)
- 2 No wall damping on NLEN
- 3 COEFVS iteration print
- 4 Buleev mixing length formula
- 5 number of pressure iterations in ADICUP
- 6 auxiliary variable printout
- 7 auxiliary variable printout
- 8 auxiliary variable printout
- 9 auxiliary variable printout
- 10 auxiliary variable printout
- 11 auxiliary variable printout
- 12 auxiliary variable printout
- 13 auxiliary variable printout
- 14 PFLOW intermediate solutions
- 15 FRAME printout
- 16 ADI convergence information
- 17 DPDXV iteration printout
- 18 printout 3 level velocity and vorticity

NOTE:

It is advisable when running the potential flow calculation for the elliptic pressure field (MODE=3,2) to add constant area extensions both upstream and downstream of the duct to be evaluated in order to minimize the effects of the upstream and downstream boundary conditions.

The output for MODE=4 presents the coefficients of the polynomial and an evaluation of the polynomial at NX points in the range from X1 to X2. Displayed are the values of the polynomial along with the first and second derivative.

```

$!L
NEQ= 6
X1= 0.0
X2= 10.0
NX= 11
XIN= 3*0.0, 3*10.0, 2*0.0
YIN= 3*0.0, 2.0, 4*0.0
ID= 0, 1, 2, 0, 1, 2, 2*0
$END
ANSWER 1 0.12000000E-03 * X** 5
ANSWER 2 -0.30000000E-02 * X** 4
ANSWER 3 0.20000000E-01 * X** 3
ANSWER 4 0.00000000 * X** 2
ANSWER 5 0.00000000 * X** 1
ANSWER 6 0.00000000 * X** 0

```

I	X	Y	YP	YPP
1	0.00000000	0.00000000	0.00000000	0.00000000
2	0.10000000E 01	0.17120000E-01	0.48600000E-01	0.86400000E-01
3	0.20000000E 01	0.11584000E 00	0.15360000E 00	0.11520000E 00
4	0.30000000E 01	0.32616000E 00	0.26460000E 00	0.10080000E 00
5	0.40000000E 01	0.63488000E 00	0.34560000E 00	0.57600000E-01
6	0.50000000E 01	0.10000000E 01	0.37500000E 00	0.27755576E-16
7	0.60000000E 01	0.13651200E 01	0.34560000E 00	-0.57600000E-01
8	0.70000000E 01	0.16738400E 01	0.26460000E 00	-0.10080000E 00
9	0.80000000E 01	0.18841600E 01	0.15360000E 00	-0.11520000E 00
10	0.90000000E 01	0.19828800E 01	0.48600000E-01	-0.86400000E-01
11	0.10000000E 02	0.20000000E 01	-0.88817842E-15	-0.66613381E-15

The output for MODE=3 provides summary tables of geometric information including the absolute value of the radius of curvature of the centerline.

JX	X	SHAPE	MAJOR AXIS	ROTATION	EXPONENT
4	0.00000000	0.10000000E 01	0.10000000E 01	0.00000000	0.20000000E 01
5	0.99000000E 00	0.10000000E 01	0.10000000E 01	0.00000000	0.20000000E 01
6	0.19800000E 01	0.10000000E 01	0.10000000E 01	0.00000000	0.20000000E 01
7	0.29700000E 01	0.10000000E 01	0.10000000E 01	0.00000000	0.20000000E 01
8	0.39600000E 01	0.10000000E 01	0.10000000E 01	0.00000000	0.20000000E 01
9	0.49500000E 01	0.10000000E 01	0.10000000E 01	0.00000000	0.20000000E 01
10	0.59400000E 01	0.10000000E 01	0.10000000E 01	0.00000000	0.20000000E 01
11	0.69300000E 01	0.10000000E 01	0.10000000E 01	0.00000000	0.20000000E 01
12	0.79200000E 01	0.10000000E 01	0.10000000E 01	0.00000000	0.20000000E 01
13	0.89100000E 01	0.10000000E 01	0.10000000E 01	0.00000000	0.20000000E 01
14	0.99000000E 01	0.10000000E 01	0.10000000E 01	0.00000000	0.20000000E 01

JX	X	CENTERLINE LOCATION (X1,X2,X3)			RAD OF CURVE
		X1	X2	X3	
4	0.00000000	0.00000000	0.00000000	0.00000000	0.00000000
5	0.99000000E 00	0.16638311E-01	0.00000000	0.99000000E 00	0.11688730E 02
6	0.19800000E 01	0.11279103E 00	0.00000000	0.19800000E 01	0.89884780E 01
7	0.29700000E 01	0.31826750E 00	0.00000000	0.29700000E 01	0.10856523E 02
8	0.39600000E 01	0.62110264E 00	0.00000000	0.39600000E 01	0.19796253E 02
9	0.49500000E 01	0.98125125E 00	0.00000000	0.49500000E 01	0.40607325E 03
10	0.59400000E 01	0.13442822E 01	0.00000000	0.59400000E 01	0.21837661E 02
11	0.69300000E 01	0.16550729E 01	0.00000000	0.69300000E 01	0.11290609E 02
12	0.79200000E 01	0.18715030E 01	0.00000000	0.79200000E 01	0.90087385E 01
13	0.89100000E 01	0.19781495E 01	0.00000000	0.89100000E 01	0.11025311E 02
14	0.99000000E 01	0.19999803E 01	0.00000000	0.99000000E 01	0.85892988E 02

Upon successful completion of writing the geometry on file #10 the following message is written:

GEOMETRY WRITTEN FROM STATION 5 AT X=0.9900E 00 TO STATION 14 AT X=0.9900E 01 FOR ITCNT= 3

The output for MODE=2 consists of intermediate printout information about the iteration followed by a tabulation of the information written on the pressure field file logical unit 13. Listed at each transverse computational plane are the stream-wise plane number, the parametric location of the centerline, the radius from the centerline of each row of grid points expressed as a fraction of the local duct radius, the azimuthal location in radians of each radial line of grid points, and a two-dimensional display of pressure coefficient, C_p , at each node used in the potential flow calculation.

```
ADI MM ITER= 1 PMAX= 0.10000E 01 DELP= 0.11584E-03 RHSMAX= 0.20776E-02 DUM1= 0.44515E-01 DUM2= 0.11151E 01
ADI MM ITER= 2 PMAX= 0.10000E 01 DELP= 0.34012E-04 RHSMAX= 0.65896E-03 DUM1= 0.41648E-01 DUM2= 0.10323E 01
ADI MM ITER= 3 PMAX= 0.10000E 01 DELP= 0.10552E-04 RHSMAX= 0.20576E-03 DUM1= 0.41174E-01 DUM2= 0.10257E 01
ADI MM ITER= 4 PMAX= 0.10000E 01 DELP= 0.32867E-05 RHSMAX= 0.64454E-04 DUM1= 0.40862E-01 DUM2= 0.10199E 01
ADI MM ITER= 5 PMAX= 0.10000E 01 DELP= 0.10287E-05 RHSMAX= 0.20220E-04 DUM1= 0.40751E-01 DUM2= 0.10175E 01
ADI MM ITER= 6 PMAX= 0.10000E 01 DELP= 0.10003E-03 RHSMAX= 0.20842E-02 DUM1= 0.38440E-01 DUM2= 0.95987E 00
ADI MM ITER= 7 PMAX= 0.10000E 01 DELP= 0.30161E-04 RHSMAX= 0.66045E-03 DUM1= 0.36932E-01 DUM2= 0.91333E 00
ADI MM ITER= 8 PMAX= 0.10000E 01 DELP= 0.93756E-03 RHSMAX= 0.20635E-03 DUM1= 0.36582E-01 DUM2= 0.90671E 00
ADI MM ITER= 9 PMAX= 0.10000E 01 DELP= 0.29228E-05 RHSMAX= 0.64658E-04 DUM1= 0.36338E-01 DUM2= 0.90406E 00
NONLINEAR INNER CONVERGENCE IN 10 ITERATIONS
ADI *** ITCNT= 6 DELP0= 0.29373E-03 DUM1= 0.29373E 00
NONLINEAR ELLIPTIC EQUATION CONVERGES IN 6 ITERATIONS
```

```
SOLUTION AT LZ= 1 1-0.29700E 01
0.00000 0.11111 0.22222 0.33333 0.44444 0.55556 0.66667 0.77778 0.88889 1.00000
0.83267D-16 0.38638 0.70867 1.0186 1.3661 1.7755 2.1230 2.4329 2.7552 3.1416
10 0.83228E-03 0.80667E-03 0.72984E-03 0.62184E-03 0.47708E-03 0.30190E-03 0.15920E-03 0.58856E-04 0.67039E-05 0.28558E-04
9 0.82123E-03 0.79608E-03 0.72064E-03 0.61454E-03 0.47224E-03 0.30001E-03 0.15962E-03 0.60859E-04 0.68895E-05 0.25206E-04
8 0.78807E-03 0.76432E-03 0.69306E-03 0.59265E-03 0.45772E-03 0.29431E-03 0.16088E-03 0.68689E-04 0.53539E-05 0.15152E-04
7 0.73351E-03 0.71197E-03 0.64736E-03 0.55610E-03 0.43313E-03 0.28398E-03 0.16183E-03 0.75570E-04 0.19054E-04 0.21460E-04
6 0.65860E-03 0.63997E-03 0.58408E-03 0.50496E-03 0.39799E-03 0.26789E-03 0.16087E-03 0.85077E-04 0.35364E-04 0.18793E-04
5 0.56439E-03 0.54921E-03 0.50369E-03 0.43916E-03 0.35158E-03 0.24454E-03 0.15595E-03 0.92993E-04 0.51697E-04 0.37932E-04
4 0.49153E-03 0.44019E-03 0.40616E-03 0.35820E-03 0.29285E-03 0.21215E-03 0.14460E-03 0.96441E-04 0.65055E-04 0.54593E-04
3 0.31981E-03 0.31250E-03 0.29057E-03 0.26082E-03 0.22055E-03 0.16892E-03 0.12418E-03 0.92483E-04 0.72659E-04 0.66051E-04
2 0.16733E-03 0.16441E-03 0.15566E-03 0.14635E-03 0.13504E-03 0.11597E-03 0.96157E-04 0.83313E-04 0.77106E-04 0.75038E-04
1 0.00000 0.53068E-05 0.21227E-04 0.49795E-04 0.86259E-04 0.11860E-03 0.14521E-03 0.16972E-03 0.18833E-03 0.19653E-03
```

```
SOLUTION AT LZ= 2 2-0.19800E 01
0.00000 0.11111 0.22222 0.33333 0.44444 0.55556 0.66667 0.77778 0.88889 1.00000
0.83267D-16 0.38638 0.70867 1.0186 1.3661 1.7755 2.1230 2.4329 2.7552 3.1416
10 0.61894E-03 0.70333E-03 0.95646E-03 0.13282E-02 0.18386E-02 0.24482E-02 0.29393E-02 0.32925E-02 0.35335E-02 0.36139E-02
9 0.64007E-03 0.72319E-03 0.97214E-03 0.13380E-02 0.18403E-02 0.24403E-02 0.29238E-02 0.32715E-02 0.35889E-02 0.35880E-02
8 0.70346E-03 0.78291E-03 0.10192E-02 0.13672E-02 0.18452E-02 0.24165E-02 0.28773E-02 0.32080E-02 0.34351E-02 0.35109E-02
7 0.80568E-03 0.87800E-03 0.10950E-02 0.14140E-02 0.18525E-02 0.23769E-02 0.28007E-02 0.31057E-02 0.33138E-02 0.33831E-02
6 0.94109E-03 0.10046E-02 0.11949E-02 0.14752E-02 0.18607E-02 0.23221E-02 0.26956E-02 0.29646E-02 0.31482E-02 0.32093E-02
5 0.11022E-02 0.11549E-02 0.13132E-02 0.15464E-02 0.18676E-02 0.22523E-02 0.25644E-02 0.27892E-02 0.29427E-02 0.29936E-02
4 0.12795E-02 0.13202E-02 0.14621E-02 0.16222E-02 0.18705E-02 0.21681E-02 0.24097E-02 0.25838E-02 0.27030E-02 0.27427E-02
3 0.14617E-02 0.14893E-02 0.15720E-02 0.16955E-02 0.18646E-02 0.20701E-02 0.22348E-02 0.23539E-02 0.24362E-02 0.24636E-02
2 0.16341E-02 0.16486E-02 0.16918E-02 0.17586E-02 0.18527E-02 0.19622E-02 0.20481E-02 0.21112E-02 0.21562E-02 0.21712E-02
1 0.17864E-02 0.17929E-02 0.18062E-02 0.18284E-02 0.18652E-02 0.19096E-02 0.19376E-02 0.19561E-02 0.19718E-02 0.19770E-02
```

```
SOLUTION AT LZ= 3 3-0.99000E 00
0.00000 0.11111 0.22222 0.33333 0.44444 0.55556 0.66667 0.77778 0.88889 1.00000
0.83267D-16 0.38638 0.70867 1.0186 1.3661 1.7755 2.1230 2.4329 2.7552 3.1416
10-0.35456E-02 0.30759E-02 0.16674E-02 0.35862E-03 0.30963E-02 0.63416E-02 0.89146E-02 0.10742E-01 0.11978E-01 0.12390E-01
9-0.33965E-02 0.29358E-02 0.15546E-02 0.43366E-03 0.31218E-02 0.63094E-02 0.88387E-02 0.10636E-01 0.11852E-01 0.12257E-01
8-0.29492E-02 0.25156E-02 0.12155E-02 0.65960E-03 0.31992E-02 0.62135E-02 0.86117E-02 0.10318E-01 0.11472E-01 0.11856E-01
7-0.22559E-02 0.18635E-02 0.68812E-03 0.10110E-02 0.33197E-02 0.60631E-02 0.82542E-02 0.98154E-02 0.10872E-01 0.11224E-01
6-0.13645E-02 0.10254E-02 0.87377E-03 0.14662E-02 0.34745E-02 0.58668E-02 0.77859E-02 0.91561E-02 0.10084E-01 0.10392E-01
5-0.32330E-03 0.45531E-04 0.78728E-03 0.19994E-02 0.36552E-02 0.56323E-02 0.72261E-02 0.83667E-02 0.91392E-02 0.93966E-02
4 0.82207E-03 0.10329E-02 0.16648E-02 0.25877E-02 0.38527E-02 0.53674E-02 0.65943E-02 0.74746E-02 0.80714E-02 0.82702E-02
3 0.20250E-02 0.21657E-02 0.25873E-02 0.32059E-02 0.40575E-02 0.50798E-02 0.59108E-02 0.65088E-02 0.69153E-02 0.70507E-02
2 0.32352E-02 0.33053E-02 0.35153E-02 0.38262E-02 0.42594E-02 0.47808E-02 0.52029E-02 0.55076E-02 0.57163E-02 0.57858E-02
1 0.44172E-02 0.44190E-02 0.44245E-02 0.44275E-02 0.44671E-02 0.45505E-02 0.45817E-02 0.45801E-02 0.45863E-02 0.45888E-02
```

```
SOLUTION AT LZ= 4 4 0.00000
0.00000 0.11111 0.22222 0.33333 0.44444 0.55556 0.66667 0.77778 0.88889 1.00000
0.83267D-16 0.38638 0.70867 1.0186 1.3661 1.7755 2.1230 2.4329 2.7552 3.1416
10-0.68654E-03 0.18027E-03 0.13361E-02 0.34925E-02 0.63766E-02 0.97245E-02 0.12320E-01 0.14148E-01 0.15375E-01 0.15783E-01
9-0.52302E-03 0.28365E-04 0.14525E-02 0.35619E-02 0.63913E-02 0.96785E-02 0.12231E-01 0.14033E-01 0.15244E-01 0.15646E-01
8-0.30049E-04 0.43299E-03 0.18178E-02 0.37971E-02 0.64642E-02 0.95680E-02 0.11987E-01 0.13701E-01 0.14853E-01 0.15236E-01
7 0.72588E-03 0.11420E-02 0.23846E-02 0.41683E-02 0.65856E-02 0.94047E-02 0.11612E-01 0.13183E-01 0.14241E-01 0.14592E-01
6 0.16863E-02 0.20440E-02 0.31104E-02 0.46483E-02 0.67465E-02 0.91990E-02 0.11129E-01 0.12511E-01 0.13442E-01 0.13750E-01
5 0.27986E-02 0.30901E-02 0.39564E-02 0.52120E-02 0.69384E-02 0.89604E-02 0.10559E-01 0.11711E-01 0.12489E-01 0.12746E-01
4 0.40148E-02 0.42349E-02 0.48865E-02 0.58353E-02 0.71528E-02 0.86977E-02 0.99231E-02 0.10814E-01 0.11161E-01 0.11614E-01
3 0.52887E-02 0.54357E-02 0.58651E-02 0.64943E-02 0.73813E-02 0.86199E-02 0.92428E-02 0.98482E-02 0.10259E-01 0.10394E-01
2 0.65706E-02 0.66436E-02 0.68531E-02 0.71618E-02 0.76136E-02 0.81412E-02 0.85526E-02 0.88610E-02 0.90726E-02 0.91407E-02
1 0.78237E-02 0.78358E-02 0.78674E-02 0.78968E-02 0.79476E-02 0.80192E-02 0.80163E-02 0.79961E-02 0.79364E-02 0.79241E-02
```

The output for MODE=1 consists of the geometric summary information shown for MODE=3. Also presented at each streamwise station are the cross sectional area of the duct and the mass flux. Two-dimensional tabulations of several parameters are also provided in the cross plane. These are:

- RADIUS - distance/YZERO from duct centerline
- THETA - angle from symmetry plane
- VEL-S - streamwise velocity /UZERO
- VEL-TH - azimuthal velocity component/UZERO in the direction of the
local azimuthal coordinate
- VEL-R - radial velocity/UZERO
- RHO - density/RZERO
- CP/2 - half the pressure coefficient
- VOR - component of the vorticity vector parallel to the centerline
- MUT - turbulent viscosity/LAMINAR VISCOSITY
- LEN - mixing length used in turbulence viscosity calculation

The output is presented for LEVEL 1, which is the results of the calculation. The only exception is for station 2 where the output is first presented at LEVEL 3, then at LEVEL 1. The LEVEL 3 output is the station 1 input which has been revised to be consistent with the governing equations.

The logical file name convention used by the code is:

- 5 Card image input
- 6 Printed output
- 8 Plot file NASA LeRC format
- 9 Scratch storage - Z array and PFLOW
- 10 Geometry for PFLOW
- 11 Restart
- 12 Restart
- 13 Pressure field

The assignment and cataloging of these files is machine and site dependant and it is the responsibility of the user to make them available to the code.

1. Report No. NASA CR-3389	2. Government Accession No.	3. Recipient's Catalog No.	
4. Title and Subtitle A THREE-DIMENSIONAL TURBULENT COMPRESSIBLE SUBSONIC DUCT FLOW ANALYSIS FOR USE WITH CONSTRUCTED COORDINATE SYSTEMS		5. Report Date APRIL 1981	6. Performing Organization Code
		8. Performing Organization Report No. 900005-F	10. Work Unit No.
7. Author(s) R. Levy, H. McDonald, W. R. Briley, and J. P. Kreskovsky		11. Contract or Grant No. NAS3-21735	
		13. Type of Report and Period Covered Contractor Report	
9. Performing Organization Name and Address Scientific Research Associates, Inc. P.O. Box 498 Glastonbury, CT 06033		14. Sponsoring Agency Code 505-04-12	
		12. Sponsoring Agency Name and Address National Aeronautics and Space Administration Washington, D.C. 20546	
15. Supplementary Notes Final report. Project Manager, Charles E. Towne, Propulsion Systems Division, NASA Lewis Research Center, Cleveland, Ohio 44135.			
16. Abstract An approximate analysis is presented for computation of three-dimensional subsonic flow in straight and curved diffusers. The development parallels that of Briley and McDonald for forward-marching solution of viscous primary and secondary flows, but differs in the coordinate formulation used and in details of the approximations. The present formulation is intended to facilitate the use of constructed coordinates in circumstances where it is difficult to maintain smooth behavior in higher derivatives. This analysis is applicable to nonorthogonal coordinate systems having a curved centerline and planar transverse coordinate surfaces normal to the centerline. The primary flow direction is taken to coincide with the local direction of the duct centerline and is hence normal to transverse coordinate planes. The formulation utilizes vector components (velocity, vorticity, transport equations) defined in terms of local Cartesian directions aligned with the centerline tangent, although the governing equations themselves are expressed in general nonorthogonal coordinates. For curved centerlines, these vector quantities are redefined in new local Cartesian directions at each streamwise location. The use of local Cartesian variables and fluxes leads to governing equations which require only first derivatives of the coordinate transformation, and this provides for the aforementioned ease in using constructed coordinates. The analysis is applied to a particular family of duct and diffuser geometries having curved centerlines and superelliptic cross sections, using a nonorthogonal constructed coordinate system. Present computed results are compared with available experimental measurements for different but related flow conditions. Qualitative agreement is observed with regard to the formation of secondary flows, migration of streamwise vortices, and distortion of the primary flow. Additional experimental data is needed to provide a basis for detailed quantitative evaluation of the analysis and flow predictions.			
17. Key Words (Suggested by Author(s)) Three-dimensional flow; Turbulent duct flow; Parabolized Navier-Stokes; Secondary flow; 3-D diffuser; Constructed coordinates		18. Distribution Statement Unclassified - unlimited STAR Category 34	
19. Security Classif. (of this report) Unclassified	20. Security Classif. (of this page) Unclassified	21. No. of Pages 39	22. Price* A03

* For sale by the National Technical Information Service, Springfield, Virginia 22161